Supporting Information

13% Efficiency Si Hybrid Solar Cells *via* Concurrent Improvement in Optical and Electrical Properties by Employing Graphene Quantum Dots

Meng-Lin Tsai,[†,‡] Wan-Rou Wei,[†] Libin Tang,[§] Hung-Chih Chang,[†] Shih-Hsiang Tai,[†] Po-Kang Yang,[†] Shu Ping Lau,[§] Lih-Juann Chen,[‡,*] and Jr-Hau He[†,*]

[†]*Computer, Electrical and Mathematical Sciences and Engineering (CEMSE) Division, King Abdullah University of Science & Technology (KAUST), Thuwal 23955-6900, Kingdom of Saudi Arabia*

[‡]*Department of Materials Science and Engineering, National Tsing Hua University, Hsinchu 30013, Taiwan, ROC*

[§]*Department of Applied Physics, The Hong Kong Polytechnic University, Hong Kong SAR*

[*]Corresponding author e-mail: jrhau.he@kaust.edu.sa; ljchen@mx.nthu.edu.tw

The comparison of integrated J_{SC} from EQE measurements and J_{SC} from *J-V* measurements.

We have made the comparison of integrated J_{SC} from EQE measurements and J_{SC} from *J-V* measurements. To compare J_{SC} obtained from *J-V* measurements with that integrated from EQE measurements, we evaluate J_{SC} from EQE by the following equation

$$J_{sc} = \int \frac{e}{hc} S(\lambda)\eta(\lambda)\lambda d\lambda \tag{1}$$

where $S(\lambda)$ is the AM 1.5G spectrum, $\eta(\lambda)$ is the measured EQE spectrum, e is the elementary electronic charge, λ is the wavelength of transmitted monochromatic light, h is the Planck constant, and c is the velocity of light in vacuum. The integrated values of J_{SC} from EQE measurements and J_{SC} from *J-V* measurements are summarized, as shown in Table S3. The results obtained by two methods exhibit slightly different values, which can be attributed to the difference in the intensity distribution of AM 1.5G spectrum between theory and experimental setups. The evaluations indicate that consistent results are obtained.

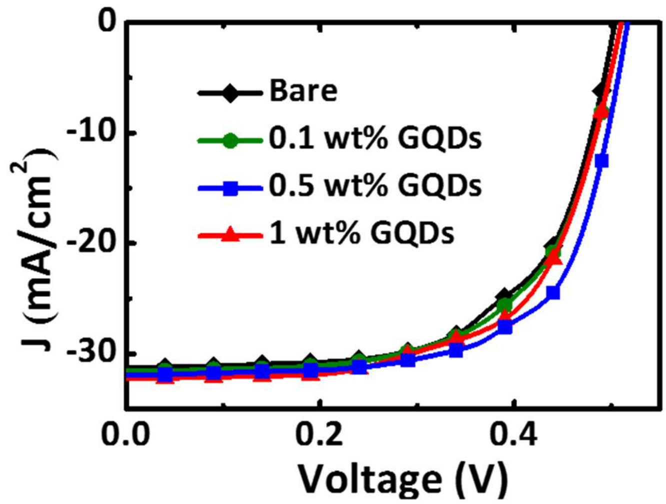

Figure S1. *J-V* characteristics of PEDOT:PSS/Si hybrid solar cells with various GQD concentrations without back surface fields.

Table S1. Photovoltaic parameters of hybrid solar cells with various GQD concentrations without back surface fields obtained from Figure S1.

GQDs	***Voc*** **(V)**	***Jsc*** **(mA/cm^2)**	***FF*** **(%)**	***PCE*** **(%)**
0 wt%	0.50	31.41	61.66	9.76
0.1 wt%	0.51	31.56	62.23	10.02
0.5 wt%	0.52	31.79	66.25	10.88
1 wt%	0.51	32.25	63.69	10.47

Table S2. Performance characteristics of Si-organic hybrid solar cells with the *PCEs* above 11%.

Structure	**Surface treatments/ Additives**	V_{oc} **(V)**	J_{sc} **(mA/cm^2)**	***FF*** **(%)**	***PCE*** **(%)**	**Ref.**
Nanocone	Back-surface doping	0.55	29.6	67.7	11.1	S1
Planar	Zonyl fluorosurfactant	0.541	29.20	71.8	11.34	S2
Hierarchical	H_2O treatment	0.52	34.46	64.06	11.48	S3
Pyramid	Back-surface doping	0.603	29.0	70.6	12.3	S4
Nanowire	TAPC intermediate layer	0.545	34.86	69.35	13.01	S5
Microdesert	Back-surface doping	0.492	36.81	66.3	12.00	S6
Planar	8-hydroxyquinolinolato-lithium	0.609	28.3	71	12.2	S7
Pyramid	Back surface doping	0.57	36.26	63.87	13.22	This work

In this table, the references are classified by years of publication. All the cells are fabricated using Si/PEDOT:PSS junction.

Table S3. The comparison of integrated J_{SC} from EQE measurements and J_{SC} from *J*-*V* measurements.

GQD Concentration (wt %)	J_{SC} Measured from *J-V* Curves (mA/cm^2)	J_{SC} Integrated from EQE Spectra (mA/cm^2)
0	**32.11**	**31.87**
0.5	**36.26**	**34.89**

References

S1. Jeong, S.; Garnett, E. C.; Wang, S.; Yu, Z.; Fan, S.; Brongersma, M. L.; McGehee, M. D.; Cui, Y. Hybrid Silicon Nanocone-Polymer Solar Cells. *Nano Lett.* **2012**, *12*, 2971-2976.

S2. Liu, Q.; Ono, M.; Tang, Z.; Ishikawa, R.; Ueno, K.; Shirai, H. Highly Efficient Crystalline Silicon/Zonyl Fluorosurfactant-Treated Organic Heterojunction Solar Cells. *Appl. Phys. Lett.* **2012**, *100*, 183901.

S3. Wei, W. R.; Tsai, M. L.; Ho, S. T.; Tai, S. H.; Ho, C. R.; Tsai, S. H.; Liu, C. W.; Chung, R. J.; He J. H. Above-11%-Efficiency Organic-Inorganic Hybrid Solar Cells with Omnidirectional Harvesting Characteristics by Employing Hierarchical Photon Trapping Structures. *Nano Lett.* **2013**, *13*, 3658-3663.

S4. Schmidt, J.; Titova, V.; Zielke, D. Organic-Silicon Heterojunction Solar Cells: Open-Circuit Voltage Potential and Stability. *Appl. Phys. Lett.* **2013**, *103*, 183901.

S5. Yu, P.; Tsai, C. Y.; Chang, J. K.; Lai, C. C.; Chen, P. H.; Lai, Y. C.; Tsai, P. T.; Li, M. C.; Pan, H. T.; Huang, Y. Y.; *et al.* 13% Efficiency Hybrid Organic/Silicon-Nanowire Heterojunction Solar Cell *via* Interface Engineering. *ACS Nano* **2013**, *7*, 10780-10787.

S6. Thiyagu, S.; Hsueh, C. C.; Liu, C. T.; Syu, H. J.; Lin, T. C.; Lin, C. F. Hybrid Organic-Inorganic Heterojunction Solar Cells with 12% Efficiency by Utilizing Flexible Film-Silicon with a Hierarchical Surface. *Nanoscale* **2014**, *6*, 3361-3366.

S7. Zhang, Y.; Zn, F.; Lee, S. T.; Liao, L.; Zhao, N.; Sun, B. Heterojunction with Organic Thin Layers on Silicon for Record Efficiency Hybrid Solar Cells. *Adv. Energy Mater.* **2014**, *4*, 1300923.